



**HAL**  
open science

## Ultra-low intensity noise, all fiber 365 W linearly polarized single frequency laser at 1064 nm

Clément Dixneuf, Germain Guiraud, Yves-Vincent Bardin, Quentin Rosa, Mathieu Goeppner, Adèle Hilico, Christophe Pierre, Johan Boulet, Nicholas Traynor, Giorgio Santarelli

► **To cite this version:**

Clément Dixneuf, Germain Guiraud, Yves-Vincent Bardin, Quentin Rosa, Mathieu Goeppner, et al.. Ultra-low intensity noise, all fiber 365 W linearly polarized single frequency laser at 1064 nm. *Optics Express*, 2020, 28, 10.1364/OE.385095 . hal-02536817

**HAL Id: hal-02536817**

**<https://hal.science/hal-02536817>**

Submitted on 8 Apr 2020

**HAL** is a multi-disciplinary open access archive for the deposit and dissemination of scientific research documents, whether they are published or not. The documents may come from teaching and research institutions in France or abroad, or from public or private research centers.

L'archive ouverte pluridisciplinaire **HAL**, est destinée au dépôt et à la diffusion de documents scientifiques de niveau recherche, publiés ou non, émanant des établissements d'enseignement et de recherche français ou étrangers, des laboratoires publics ou privés.



# Ultra-low intensity noise, all fiber 365 W linearly polarized single frequency laser at 1064 nm

CLÉMENT DIXNEUF,<sup>1,2,\*</sup>  GERMAIN GUIRAUD,<sup>2</sup> YVES-VINCENT BARDIN,<sup>2</sup> QUENTIN ROSA,<sup>2</sup> MATHIEU GOEPNER,<sup>2</sup> ADÈLE HILICO,<sup>1</sup> CHRISTOPHE PIERRE,<sup>3</sup> JOHAN BOULLET,<sup>3</sup> NICHOLAS TRAYNOR,<sup>2</sup> AND GIORGIO SANTARELLI<sup>1</sup> 

<sup>1</sup>LP2N, IOGS, CNRS and Université de Bordeaux, rue François Mitterrand, 33400 Talence, France

<sup>2</sup>Azur Light Systems, 11 Avenue de Canteranne, 33600 Pessac, France

<sup>3</sup>ALPhANOV, rue François Mitterrand, 33400 Talence, France

\*cdixneuf@azurlight-systems.com

**Abstract:** We demonstrate a robust linearly polarized 365 W, very low amplitude noise, single frequency master oscillator power amplifier at 1064 nm. Power scaling was done through a custom large mode area fiber with a mode field diameter of 30  $\mu\text{m}$ . No evidence of stimulated Brillouin scattering or modal instabilities are observed. The relative intensity noise is reduced down to  $-160$  dBc/Hz between 2 kHz and 10 kHz via a wide band servo loop (1 MHz bandwidth). We achieve 350 W of isolated power, with a power stability  $< 0.7\%$  RMS over 1100 hours of continuous operation and a near diffraction limited beam ( $M^2 < 1.1$ ).

© 2020 Optical Society of America under the terms of the [OSA Open Access Publishing Agreement](#)

## 1. Introduction

With the advances in fundamental science such as gravitational wave detection (GWD) [1,2] or cold atom science [3] and high-end industry (e.g. functional quantum calculators [4]), the need for single frequency (SF) high-power fiber lasers has been increasing over the last decade. The ability to maintain an excellent modal quality, the wide tuning range in the Ytterbium (Yb) band [5–8], the linear polarization and the optical low-noise operation is driving this technology as an excellent replacement for more established high-power bulk systems in the 1  $\mu\text{m}$  region.

Although very high-power fiber lasers have been demonstrated in a master oscillator power amplifier (MOPA) configuration [9], SF operation faces some physical limitations, stimulated Brillouin scattering (SBS) being the principal one. This well-known non-linear effect results from the interaction between optical photons and acoustic phonons, creating a backscattered signal [10]. This has an impact on amplifier intensity noise and will eventually lead to catastrophic system damage at high enough power.

Several groups have already demonstrated SF operation up to hundreds of watts of continuous power. Robin et al., have reported 811 W SF output power using photonic crystal fiber [11]. They used a free space counter-propagative pump configuration to amplify the 1064 nm signal, but it is known that with this technique, SBS threshold is almost two times bigger than with co-propagative pump scheme [12]. In 2017, Huang et al., published for the first time 414 W of SF radiation, in an all-fiber design [13]. They used a Large Mode Area (LMA) fiber with a core diameter of 25  $\mu\text{m}$ . To avoid SBS, they applied a strain gradient, inducing a broadening of the Brillouin gain spectra. By this technique, they improved the SBS threshold by at least four times. The use of tapered amplifiers has also allowed to reach high continuous power with free space pumping [14–17]. For those configurations, the use of free space coupling or implementing calibrated strains along the active fiber are less compatible with industrial laser standards relying on robustness and reliability. Focusing on an architecture without any management of SBS, Ma et al. [18] have developed a 332 W all-fiber MOPA with, as a final gain fiber, an LMA Yb-doped

fiber (YDF) with a core of  $30\ \mu\text{m}$  and at the output an  $M^2$  of 1.4. However, none of these studies have focused on the noise characteristics of the amplifiers or the long-term stability of these systems.

More recently, Buikema et al. [19] and Wellmann et al. [20] proposed SF amplifiers using commercial fibers delivering respectively 178 W and 200 W of low noise optical power, suitable for next generation of GWD. In-depth investigations on the modal content or beam jitter shown that LMA fibers can guide highly stable beams with 95% of the power contained in the fundamental TEM<sub>00</sub> mode. It is noticeable that in [20], the fiber is coiled in two parts to create a thermal gradient aiming to increase the SBS threshold. In addition, it is in a counter-propagative configuration with a free space injection of the signal in the final amplifier, adding complexity in the system.

## 2. Design of the MOPA system

In this paper, in addition to focusing on power scaling in a fully all fiber system, we investigate the intensity noise and reduce it to  $-160\ \text{dBc/Hz}$  via a wideband servo loop. We report here 365 W of output power, using a custom LMA Yb-doped fiber, with a relative intensity noise (RIN) below  $-149\ \text{dBc/Hz}$  at 5 MHz and a power stability  $< 0.7\%$  RMS over nearly 1100 h of continuous operation. The laser architecture, shown in Fig. 1, is based on an external cavity laser diode (ECLD) seeding a MOPA in a three stages configuration.

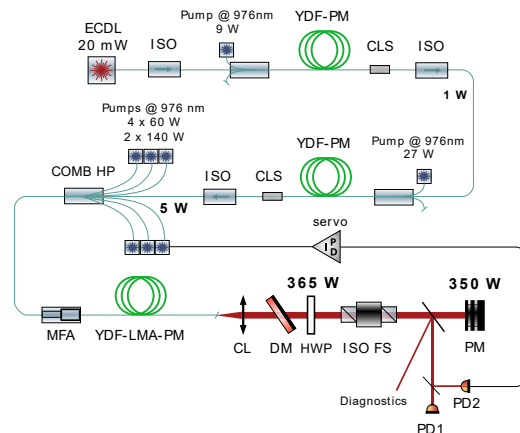


**Fig. 1.** Global scheme of the amplifier. ISO : optical-fiber isolator ; CLS : cladding-light stripper ; COMB HP : high-power combiner ; CL : collimation lens ; DM : dichroic mirror ; HWP : half-wave plate ; ISO FS : free space isolator ; PM : power meter ; PD1 : out-of-loop photodiode ; PD2 : in-loop photodiode

### 2.1. Seed laser and pre-amplifiers

The seed laser delivers 20 mW of linearly polarized light at 1064 nm with a linewidth  $< 30\ \text{kHz}$ . This measure is estimated by a heterodyne beat note signal with narrow linewidth SF laser ( $< 10\ \text{kHz}$ ). The ECLD is protected from optical feedback from the other amplification stages by a fiber isolator. The signal is pre-amplified up to 5 W through two preamplifiers, composed of double-clad YDF-PM-10/125  $\mu\text{m}$  diameter fibers, 2.5 m each, having a clad absorption coefficient around 5 dB/m at 976 nm. In both stages, the residual cladding light is suppressed by a cladding mode stripper and fiber isolators are placed at the end of each preamplifiers. At the end of the

main preamplifier, the optical signal-to-noise ratio (OSNR) is  $> 55$  dB (0.05 nm bandwidth) and the RIN is at  $-155$  dBc/Hz at 5 MHz. The first two stages are pumped respectively by 9 W and 27 W pump diodes at 976 nm.

## 2.2. Main amplifier

The 5 W pre-amplified signal is then injected in a  $(6 + 1) \times 1$  fiber combiner. The available pump sources ( $4 \times 60$  W and  $2 \times 140$  W) and the signal are injected into the 10/125  $\mu\text{m}$  diameter double clad output fiber of the combiner. In order to optimize the injection into the PM-LMA fiber, a mode field adapter (MFA) [21,22] has been developed to match the mode field diameter (MFD) of the combiner and active fiber. The active fiber has been custom developed with an MFD of 30  $\mu\text{m}$ , a numerical aperture of 0.055 and a pump cladding absorption of 12 dB/m @ 976 nm. Taking into account the strong absorption coefficient and the emission wavelength, we used a length of 2 m. The output of the active fiber has been angle cleaved at  $8^\circ$  to avoid back reflections. The residual pump is removed using a high reflectivity (HR) dichroic mirror. The final amplifier has been carefully coiled on a water-cooled aluminum plate while monitoring the beam shape and minimizing the power contained into the clad. At last, the output beam is collimated at a diameter of 3 mm and passes through a free space isolator providing a linearly polarized beam. The polarization at the input of the isolator is adjusted by a half-wave plate.

## 3. Power scaling and analysis of the laser

### 3.1. Output power and optical spectrum

The output power versus pump power is plotted in Fig. 2(a). We reach 365 W, with a pump to signal conversion efficiency of 80% and the linearly polarized power after the isolator is 350 W (77% system efficiency). The estimated polarization extinction ratio (PER) is about 17 dB. During the power scaling process, the optical spectra, shown in Fig. 2(b), exhibits an OSNR  $> 50$  dB (0.05 nm bandwidth). The spectra were measured after the injection of 10 mW of sampled signal into a single mode fiber in an Advantest Q8384.

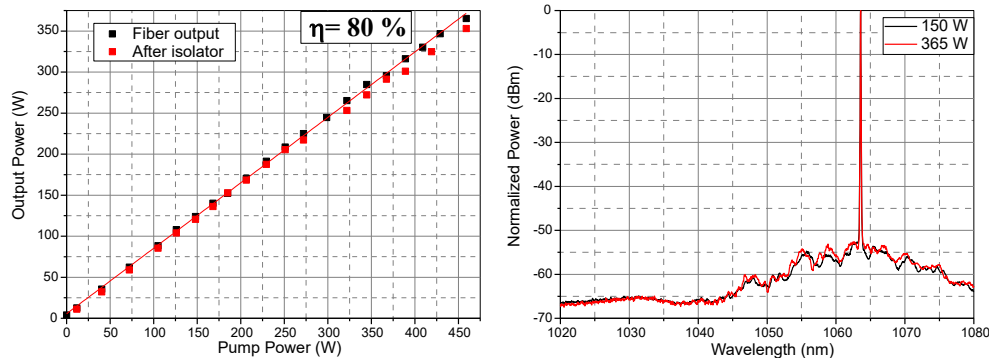


**Fig. 2.** (a) : on the left, output power versus pump power at the fiber output (black dots) showing 80% efficiency and after the isolator (red dots), (b) : on the right, optical spectra of the laser at 150 W and 365 W exhibiting more than 50 dB of OSNR (0.05 nm bandwidth).

### 3.2. Optical noise characteristics

#### 3.2.1. SBS investigation

The main limitation in power scaling of SF amplifier systems is the onset of SBS. There are several approaches to detect this non-linear effect, such as the monitoring of the backward power

via a coupler or the high Fourier frequencies ( $>$  few MHz) RIN measurements [12,18]. In order to investigate the threshold of SBS, we measured the RIN from low to high output powers.

The RIN is plotted on Fig. 3. For each measurement, we sampled around 14 mW of optical signal detected by a 3 mm diameter InGaAs photodiode to obtain about 10 mA of photocurrent. The photocurrent is then converted and amplified through a low noise electronic circuit and processed by a vector signal analyzer (VSA, HP89410A) for FFT measurements. With 14 mW of optical power, the detection noise is around  $-163$  dBc/Hz. The RIN at 5 MHz is constant from 150 W to 365 W (see inset), indicating that the system remains below the Brillouin threshold. There is a slight increase in noise from 50W to 150W, which we believe is related to the influence of residual cladding modes. For an undoped fiber with the same geometry we would expect to observe the onset of Brillouin scattering below 200 W. We think that the strong thermal gradient in the short length of doped fiber acts to broaden the Brillouin gain profile to push the SBS limit to higher powers.

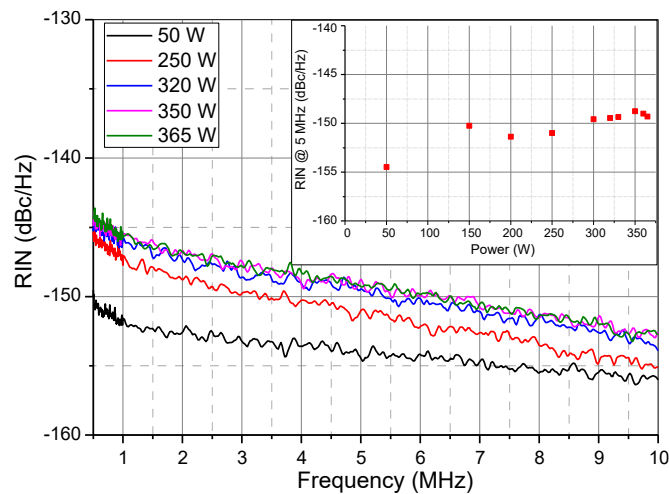


**Fig. 3.** RIN measurements, showing no sign of SBS (lines) (inset) RIN level measured at 5 MHz (red squares) versus output power.

The fundamental question of frequency noise in fiber amplifiers has been investigated many times [19,20,23,24]. Apart from low frequency noise added from thermal and mechanical fluctuations, degradation of frequency noise in the amplification process is not expected but was not tested.

### 3.2.2. Intensity noise control

To improve the RIN at Fourier frequencies  $<$  1 MHz, we have implemented a feedback control of the intensity noise, leading to a reduction of the RIN below  $-150$  dBc/Hz between 1 kHz and 500 kHz and at  $-160$  dBc/Hz between 2 kHz and 10 kHz.

It is known that the amplification process induces an excess of noise, especially at low frequencies, where the pump amplitude noise is converted in signal amplitude noise [25,26]. Different noise reduction techniques have been demonstrated in the past, one based on free-space acousto-optic modulators (AOM), but the one qualified for very high-power systems have a bandwidth limited at 100 kHz because of the inherent time delay [27,28]. The servo system we developed is an upgraded version of the one used by Zhao et al. [29], where a control current is directly added to the pump drivers, with a wide control bandwidth ( $>$  1 MHz). The two photodetectors are illuminated almost equally, leading to a total detection noise of  $-161$

dBc/Hz. Apart from the servo peak, the noise level remains below  $-140$  dB/Hz at all frequencies from 300 Hz to 10 MHz and is reduced to  $-160$  dB/Hz from 2 to 10 kHz. The spikes that we see on Fig. 4. are due to the high-power pump diodes power supply and can be removed by an optimization of all the electronical components. This large wideband control is a key factor for atomic physics [30].

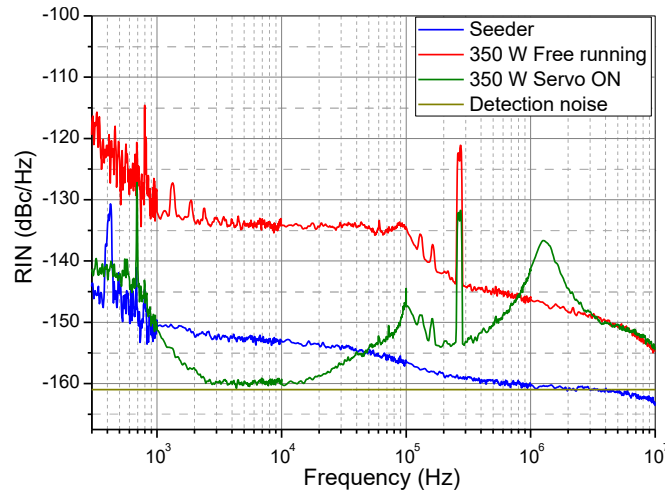


**Fig. 4.** Performance of the feedback loop on the amplifier (green) compared to free-running noise (red) and the noise of the seeder (blue)

### 3.3. Modal stability and Photodarkening investigation

It is well known that LMA fibers can suffer from transverse modal instability (TMI) or photodarkening induced modal degradation. TMI has been extensively studied [31], but photodarkening induced modal degradation has been identified more recently [32–34]. This phenomenon leads to a power roll-over combined with an increase of cladding light during photodarkening process. From this point of view, long term fiber degradation is more important than just the loss of signal power as it can strongly impact the modal content of the output.

While the subject of TMI is not a main focus of this work, we can offer some indications as to why we believe that TMI is not reached in this case with respect to the current scientific consensus on the subject.

First of all, it seems to be widely accepted that the main physical parameter driving TMI is thermal load and thermal gradients within the optical fiber. From this point of view, our system compares very favorably with many other systems in several important aspects. The absolute efficiency of this fiber is very high. The slope efficiency with respect to launched pump power is 80%, and when the unabsorbed pump power (19 W) is removed, the slope efficiency increases to 83%. Allowing for approximately 2% loss in collimating lens and dichroic filter, the absolute efficiency is estimated to be 85-86%, which is very close to the maximum theoretical value of 92% with respect to pump and signal wavelengths.

In addition, we have accurately evaluated the photodarkening effect by monitoring the output power on amplifier using a pristine fiber. The fiber exhibits nearly undetectable photodarkening, the measurement resolution is about 1% when considering all the experimental parameters. This means that no excess thermal load is induced via this phenomenon. Past experiences have shown that photodarkening can strongly enhance mode degradation on LMA fibers [35]. The fiber used

in this reference, with similar general properties to the fiber used here, was stable above 200 W of output power for a “pristine” optical fiber. However, the photodarkening was shown to strongly effect the threshold of modal degradation.

Even if current theories [36 and references therein] have not determined a clear parameter-set or a maximal thermal load relating to the onset of TMI applicable to specific fiber geometries, an estimation of around 34 W/m was made by Jauregui et al. in the case of a fiber with significant photodarkening [37]. The authors also stated that the presence of photodarkening is estimated to reduce the TMI threshold by at least a factor of two, indicating around 70 W/m for a fiber limited by quantum defect heating (as it is our case). In our case, taking into account absorbed pump power, the thermal load of our fiber is 35 W/m, which according to the above work would be above the TMI limit if photodarkening was present, but comfortably below the limit where the system is dominated by quantum defect heating.

Another aspect which seems to have an observable influence on TMI threshold is the quality of fundamental mode excitation. In this respect we ensure extremely good mode field matching which should significantly reduce the risks of early onset TMI.

We have thus studied potential TMI by using the method described by Otto et al. [31] and observed on RIN measurements by Karow et al. [38]. A mask with 3 holes has been placed in the beam path in front of the photodiode. If TMI occurs, either discrete peaks are expected due to mode oscillations leading to the occurrence of discrete intensity peaks in the [500 Hz – 5 kHz] range or a broadband increase if the chaotic oscillation regime is reached. On Fig. 5., despite some low frequency noise increase (below 1 kHz) due to the measurement set-up not degradation both in the RIN power spectral density nor in the time domain are observed.

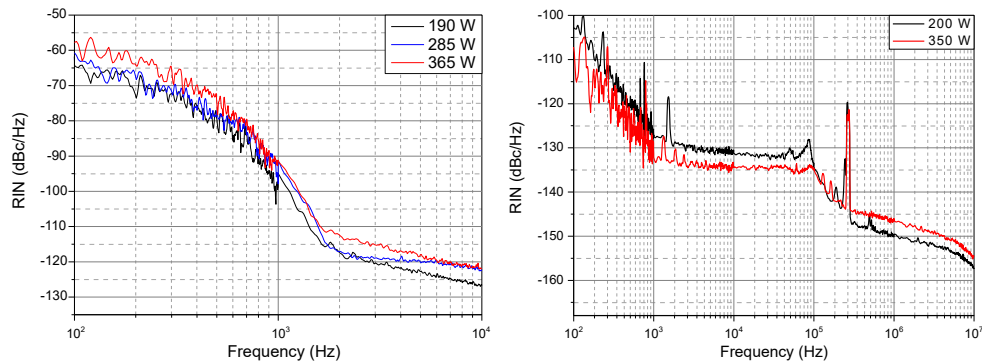


**Fig. 5.** (a): on the left, RIN Measurement with a 3-hole mask in front of the photodiode at different output optical powers. (b): on the right, RIN at the output of the isolator at various optical powers

We believe that another evidence of TMI absence comes from the extremely good behavior of the servo loop that would be impaired by TMI onset due to the intrinsic inhomogeneities of both feedback and out-of-loop photodiodes.

### 3.4. Beam quality and power stability

Beam quality is an important parameter in high power lasers. Such LMA fibers are known to have a good modal content, where the TEM<sub>00</sub> mode contains more than 95% of the power [19,20,29].

The  $M^2$  measurement plotted on Fig. 6. is below 1.1 on both optical axes. This analysis proves that even if the fiber used is not strictly single mode, it keeps a diffraction limited behavior.

Reliability is essential for high end applications. A long-time continuous operation of the laser, plotted on Fig. 7., has been done during nearly 1100 h in addition to more than 200 additional

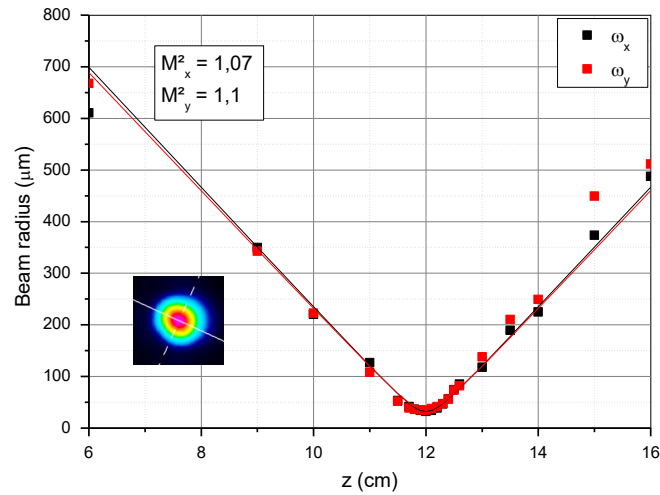


**Fig. 6.** Amplifier  $M^2$  measurement at full power with  $M_x^2 = 1.07$  and  $M_y^2 = 1.1$

hours of total operation during testing and measurement of the system. The output power is stable, with no sign of long-term degradation and excellent stability on the polarized output.

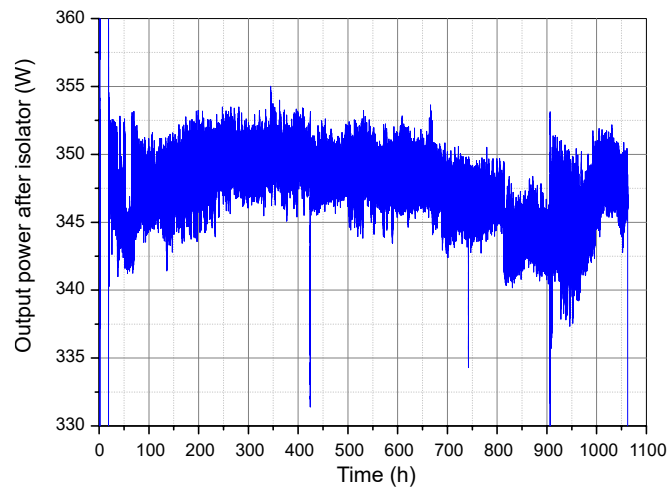


**Fig. 7.** Long time power stability measurement after isolator during about 1100 hours.

In order to better analyze this long-term time series, we have processed the data using the Allan deviation, a statistical tool widely used by the time and frequency community [39] and more recently applied to the characterization of the optical power stability [40]. Figure 8. shows the Allan deviation (log-log plot) of the power fluctuations expressed in percent of the normalized optical power respect to the measurement time.

The plotted Allan deviation shows that the RMS fluctuation is below 0.2 percent for measurement times between 10 s and  $10^5$  s. This quantifies well the very good stability for this high-power system. This is, in our knowledge, the longest continuous operation ever reported in the single

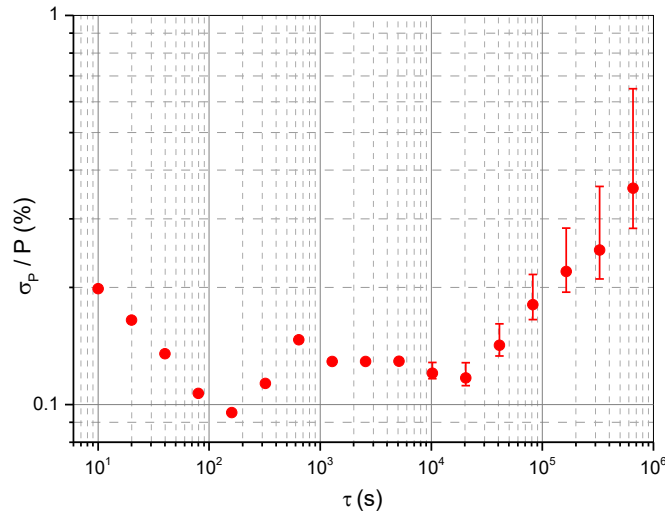


**Fig. 8.** Log-log plot of the Allan deviation of the power fluctuations expressed in percent of the total optical power.

frequency regime at 1064 nm at this level of power. In addition, no degradation of the mode has been observed. This proves that this amplifier system is suitable to be used in high power scientific and industrial systems that require robustness and reliability.

#### 4. Conclusion

We have developed an ultra-low-noise fiber amplifier, delivering up to 365 W of linearly polarized power with a diffraction limited beam ( $M^2 < 1.1$ ), only limited by the pump power available. Parasitic effects such as SBS or TMI have been one of the focus of this paper but none of them were present in our system. The good thermal management of the fiber and the pumps allowed us to prove the excellent stability of the system during about 1100 hours, showing no sign of degradation. In addition, the active fiber length could be reduced at least by 25% while keeping an efficiency  $> 75\%$  and an OSNR  $> 50$  dB. This paves the way to a power scaling up to half a kW of low noise continuous optical power with the same architecture. With further investigations on the modal content and the beam jitter, the amplifier would be a good candidate for advanced gravitational wave detectors.

#### Funding

Agence Nationale de la Recherche (LAB COM - 17 LCCO 0002 01); Conseil Régional Aquitaine (2017-1R50302-00013493); LAPHIA; Association Nationale de la Recherche et de la Technologie (ANRT 2018/0102).

#### Acknowledgment

We thank the technical team of the laboratory, P. Teulat and J-H. Codarbox, for the mechanical and an electronical support.

#### Disclosures

The authors declare no conflicts of interest.

## References

1. LIGO Scientific Collaboration, "Advanced Virgo: a second-generation interferometric gravitational wave detector," *Classical Quantum Gravity* **32**(2), 024001 (2015).
2. LIGO Scientific Collaboration and Virgo Collaboration, "Observation of Gravitational Waves from a Binary Black Hole Merger," *Phys. Rev. Lett.* **116**(6), 061102 (2016).
3. J. Hu, L. Zhang, H. Liu, K. Liu, Z. Xu, and Y. Feng, "High power room temperature 1014.8 nm Yb fiber amplifier and frequency quadrupling to 253.7 nm for laser cooling of mercury atoms," *Opt. Express* **21**(25), 30958 (2013).
4. M. Anderlini, P. J. Lee, B. L. Brown, J. Sebby-Strabley, W. D. Phillips, and J. V. Porto, "Controlled exchange interaction between pairs of neutral atoms in an optical lattice," *Nature* **448**(7152), 452–456 (2007).
5. J. Wu, X. Zhu, H. Wei, K. Wiersma, M. Li, J. Zong, A. Chavez-Pirson, V. Temyanko, L. J. LaComb, R. A. Norwood, and N. Peyghambarian, "Power scalable 10 W 976 nm single-frequency linearly polarized laser source," *Opt. Lett.* **43**(4), 951 (2018).
6. N. Valero, C. Feral, J. Lhermite, S. Petit, R. Royon, Y.-V. Bardin, J. Bouillet, A. Proulx, Y. Taillon, and E. Cormier, "29W diffraction limited monolithic ytterbium doped fiber laser system operating at 976 nm in the continuous wave regime," in *2019 Conference on Lasers and Electro-Optics Europe and European Quantum Electronics Conference (2019)*, Paper Cj\_13\_4 (Optical Society of America, 2019), p. cj\_13\_4.
7. B. Gouhier, S. Rota-Rodrigo, G. Guiraud, N. Traynor, and G. Santarelli, "Low-noise single-frequency 50 W fiber laser operating at 1013 nm," *Laser Phys. Lett.* **16**(4), 045103 (2019).
8. B. Gouhier, G. Guiraud, S. Rota-Rodrigo, J. Zhao, N. Traynor, and G. Santarelli, "25 W single-frequency, low noise fiber MOPA at 1120 nm," *Opt. Lett.* **43**(2), 308 (2018).
9. E. A. Shcherbakov, V. V. Fomin, A. A. Abramov, A. A. Ferin, D. V. Mochalov, and V. P. Gapontsev, "Industrial grade 100kW power CW fiber laser," in *Advanced Solid-State Lasers Congress* (OSA, 2013), p. AT4A.2.
10. N. A. Brilliant, "Stimulated Brillouin scattering in a dual-clad fiber amplifier," *J. Opt. Soc. Am. B* **19**(11), 2551–2557 (2002).
11. C. Robin, I. Dajani, and B. Pulford, "Modal instability-suppressing, single-frequency photonic crystal fiber amplifier with 811 W output power," *Opt. Lett.* **39**(3), 666 (2014).
12. M. Hildebrandt, S. Buesche, P. Wessels, M. Frede, and D. Kracht, "Brillouin scattering spectra in high-power single-frequency ytterbium doped fiber amplifiers," *Opt. Express* **16**(20), 15970 (2008).
13. L. Huang, H. Wu, R. Li, L. Li, P. Ma, X. Wang, J. Leng, and P. Zhou, "414 W near-diffraction-limited all-fiberized single-frequency polarization-maintained fiber amplifier," *Opt. Lett.* **42**(1), 1 (2017).
14. A. I. Trikshev, A. S. Kurkov, V. B. Tsvetkov, S. A. Filatova, J. Kerttula, V. Filippov, Y. K. Chamorovskiy, and O. G. Okhotnikov, "A 160 W single-frequency laser based on an active tapered double-clad fiber amplifier," *Laser Phys. Lett.* **10**(6), 065101 (2013).
15. V. Filippov, Y. Chamorovskii, J. Kerttula, K. Golant, M. Pessa, and O. G. Okhotnikov, "Double clad tapered fiber for high power applications," *Opt. Express* **16**(3), 1929 (2008).
16. V. Filippov, Y. Chamorovskii, J. Kerttula, A. Kholodkov, and O. G. Okhotnikov, "Single-mode 212 W tapered fiber laser pumped by a low-brightness source," *Opt. Lett.* **33**(13), 1416 (2008).
17. C. Pierre, G. Guiraud, C. Vincont, N. Traynor, G. Santarelli, and J. Bouillet, "120W single frequency laser based on short active double clad tapered fiber," in *2017 European Conference on Lasers and Electro-Optics and European Quantum Electronics Conference*, (Optical Society of America, 2017), paper CJ\_9\_3.
18. P. Ma, P. Zhou, Y. Ma, R. Su, X. Xu, and Z. Liu, "Single-frequency 332 W, linearly polarized Yb-doped all-fiber amplifier with near diffraction-limited beam quality," *Appl. Opt.* **52**(20), 4854 (2013).
19. A. Buikema, F. Jose, S. J. Augst, P. Fritschel, and N. Mavalvala, "Narrow-linewidth fiber amplifier for gravitational-wave detectors," *Opt. Lett.* **44**(15), 3833 (2019).
20. F. Wellmann, M. Steinke, F. Meylahn, N. Bode, B. Willke, L. Overmeyer, J. Neumann, and D. Kracht, "High power, single-frequency, monolithic fiber amplifier for the next generation of gravitational wave detectors," *Opt. Express* **27**(20), 28523 (2019).
21. X. Zhou, Z. Chen, H. Zhou, and J. Hou, "Mode-field adaptor between large-mode-area fiber and single-mode fiber based on fiber tapering and thermally expanded core technique," *Appl. Opt.* **53**(22), 5053 (2014).
22. P. Hofmann, A. Mafi, C. Jollivet, T. Tiess, N. Peyghambarian, and A. Schulzgen, "Detailed Investigation of Mode-Field Adapters Utilizing Multimode-Interference in Graded Index Fibers," *J. Lightwave Technol.* **30**(14), 2289–2298 (2012).
23. I. Ricciardi, S. Mosca, P. Maddaloni, L. Santamaria, M. De Rosa, and P. De Natale, "Phase noise analysis of a 10Watt Yb-doped fibre amplifier seeded by a 1-Hz-linewidth laser," *Opt. Express* **21**(12), 14618–14626 (2013).
24. N. Chiodo, K. Djerroud, O. Acef, A. Clairon, and P. Wolf, "Lasers for coherent optical satellite links with large dynamics," *Appl. Opt.* **52**(30), 7342 (2013).
25. H. Tünnermann, J. Neumann, D. Kracht, and P. Weßels, "Gain dynamics and refractive index changes in fiber amplifiers: a frequency domain approach," *Opt. Express* **20**(12), 13539 (2012).
26. J. Zhao, G. Guiraud, F. Floissat, B. Gouhier, S. Rota-Rodrigo, N. Traynor, and G. Santarelli, "Gain dynamics of clad-pumped Yb-fiber amplifier and intensity noise control," *Opt. Express* **25**(1), 357 (2017).
27. J. Junker, P. Oppermann, and B. Willke, "Shot-noise-limited laser power stabilization for the AEI 10 m Prototype interferometer," *Opt. Lett.* **42**(4), 755 (2017).

28. P. Kwee, C. Bogan, K. Danzmann, M. Frede, H. Kim, P. King, J. Pöld, O. Puncken, R. L. Savage, F. Seifert, P. Wessels, L. Winkelmann, and B. Willke, "Stabilized high-power laser system for the gravitational wave detector advanced LIGO," *Opt. Express* **20**(10), 10617 (2012).
29. J. Zhao, G. Guiraud, C. Pierre, F. Floissat, A. Casanova, A. Hreibi, W. Chaibi, N. Traynor, J. Bouillet, and G. Santarelli, "High-power all-fiber ultra-low noise laser," *Appl. Phys. B* **124**(6), 114 (2018).
30. M. E. Gehm, K. M. O'Hara, T. A. Savard, and J. E. Thomas, "Dynamics of noise-induced heating in atom traps," *Phys. Rev. A* **58**(5), 3914–3921 (1998).
31. H.-J. Otto, F. Stutzki, F. Jansen, T. Eidam, C. Jauregui, J. Limpert, and A. Tünnermann, "Temporal dynamics of mode instabilities in high-power fiber lasers and amplifiers," *Opt. Express* **20**(14), 15710 (2012).
32. H.-J. Otto, N. Modsching, C. Jauregui, J. Limpert, and A. Tünnermann, "Impact of photodarkening on the mode instability threshold," *Opt. Express* **23**(12), 15265 (2015).
33. B. Ward, "Theory and modeling of photodarkening-induced quasi static degradation in fiber amplifiers," *Opt. Express* **24**(4), 3488 (2016).
34. J. Bouillet, C. Vinçont, C. Aguegaray, and A. Jolly, "Regime-dependent photo-darkening-induced modal degradation in high power fiber amplifier," in *Lasers Congress 2016 (ASSL, LSC, LAC)* (OSA, 2016), p. ATu4A.3.
35. A. V. Shubin, M. V. Yashkov, M. A. Melkumov, S. A. Smirnov, I. A. Bufetov, and E. M. Dianov, "Photodarkening of alumosilicate and phosphosilicate Yb-doped fibers," in *2007 European Conference on Lasers and Electro-Optics and the International Quantum Electronics Conference* (2007), pp. 1.
36. M. N. Zervas, "Transverse mode instability, thermal lensing and power scaling in Yb<sup>3+</sup>-doped high-power fiber amplifiers," *Opt. Express* **27**(13), 19019 (2019).
37. C. Jauregui, H.-J. Otto, F. Stutzki, J. Limpert, and A. Tünnermann, "Simplified modelling the mode instability threshold of high power fiber amplifiers in the presence of photodarkening," *Opt. Express* **23**(16), 20203 (2015).
38. M. Karow, H. Tünnermann, J. Neumann, D. Kracht, and P. Weßels, "Beam quality degradation of a single-frequency Yb-doped photonic crystal fiber amplifier with low mode instability threshold power," *Opt. Lett.* **37**(20), 4242 (2012).
39. D. W. Allan and J. Levine, "A Historical Perspective on the Development of the Allan Variances and Their Strengths and Weaknesses," *IEEE Trans. Ultrason., Ferroelect., Freq. Contr.* **63**(4), 513–519 (2016).
40. F. Tricot, D. H. Phung, M. Lours, S. Guérandel, and E. de Clercq, "Power stabilization of a diode laser with an acousto-optic modulator," *Rev. Sci. Instrum.* **89**(11), 113112 (2018).